Invariant-mass spectrum of ^{11}O

T. B. Webb, R. J. Charity ⬡, J. M. Elson, D. E. M. Hoff, C. D. Pruitt, and L. G. Sobotka
Departments of Chemistry and Physics, Washington University, St. Louis, Missouri 63130, USA

K. W. Brown, J. Barney, G. Cerizza, J. Estee, W. G. Lynch, J. Manfredi, P. Morfouace ⬡, C. Santamaria, S. Sweany,
M. B. Tsang, T. Tsang, Y. Zhang ⬡, and K. Zhu
National Superconducting Cyclotron Laboratory, Michigan State University, East Lansing, Michigan 48824, USA

S. A. Kuvin, D. McNeel, J. Smith ⬡, and A. H. Wuosmaa
Department of Physics, University of Connecticut, Storrs, Connecticut 06269, USA

Z. Chajecki
Department of Physics, Western Michigan University, Kalamazoo, Michigan 49008, USA

The invariant-mass distribution of ^{11}O fragments formed in two-neutron-knockout reactions with a ^{13}O projectile and ^{9}Be target has been further examined. Gating on events where the ^{9}C decay fragments produced following $2p$ emission are recoiled transversely in the projectile's frame improves the overall invariant-mass resolution. The observed peak is now shown to have contributions from at least two ^{11}O levels, in contradiction with the suggestion of Fortune [Phys. Rev. C **99**, 051302(R) (2019)]. The data, however, do not differentiate between the ground-state properties obtained by the Gamow coupled-channels calculation and the prompt $2p$-decay model of Fortune. The ground-state $2p$-decay energy is 4.25(6) MeV in a two-level fit to the data, but lower values are possible if more states contribute to the observed spectrum, as suggested in the previous analysis.

In a recent experiment, the invariant-mass technique was used to make the first observation of ^{11}O [1] and produce a high-statistics spectrum of ^{12}O states [2]. These particle-unbound states were produced from double- and single-neutron-knockout reactions with an ^{13}O projectile. The invariant-mass spectrum for ^{11}O contained a wide peak which was interpreted with the aid of Gamow coupled-channel (GCC) calculations as a multiplet with contributions from fours states: $3/2_1^-$, $3/2_2^-$, $5/2_1^+$, and $5/2_2^+$. Subsequently, Fortune disagreed with this interpretation and suggested that the observed peak is largely from the ground state $(3/2_1^-)$ alone [3]. His interpretation was based on his calculation of a much larger ground-state decay width compared with the GCC value. In an additional paper [4], Fortune further suggested that, based on a simple model of the overlap between the structures of the ^{13}O projectile and the ^{11}O states, only the ground state should be populated with any significant yield. In light of these issues we further examine the experimental data.

The GCC is a state-of-the-art structure model that treats bound and continuum effects on an equal footing [5]. Coupling between shell-model states and the continuum can modify the predicted configuration, especially in the vicinity of a threshold. For ^{11}O, the calculation has two protons interacting with a deformed ^{9}C core. Fortune calculated the decay width using a more traditional technique [3,6]. He calculated a decay width of 1.6 MeV from sequential decays

through the lowest 1^-, 2^-, 1^+, and 2^+ states of ^{10}N. He also calculated a decay width of 2.46 MeV from the simultaneous emission of both two p-shell protons and two sd-shell protons. Fortune suggested that the width of the experimental peak is consistent with the simultaneous-decay prediction alone. The GCC model does not specifically consider simultaneous and sequential $2p$-decay processes, but rather calculates the total decay width in a more general framework which allows for more complex decay patterns [7].

The experiment was performed at the National Superconducting Cyclotron Laboratory at Michigan State University, which provided a secondary beam of ^{13}O at $E/A = 69.5$ MeV. This beam bombarded a 193-mg/cm^2-thick Be target. Charged particles produced in reactions between the target and projectile were detected in the High Resolution Array (HiRA) [8]. More details can be found in Refs. [1,2]. Low-lying ^{11}O states undergo $2p$ decay and the invariant-mass spectrum is constructed from detected $2p + {}^{9}$C coincidence events [1]. The $2p$-decay energy E_T was determined from the measured invariant mass of these events and the spectrum for all detected events was presented in Ref. [1] and is also shown in Fig. 1(a). A small background subtraction from events where ^{10}C and ^{11}C are misidentified as ^{9}C was made (see Ref. [1] for details).

The previous decomposition of this peak into contributions from the two lowest $3/2^-$ and $5/2^+$ states and a smooth background is also shown by the curves. The relative location
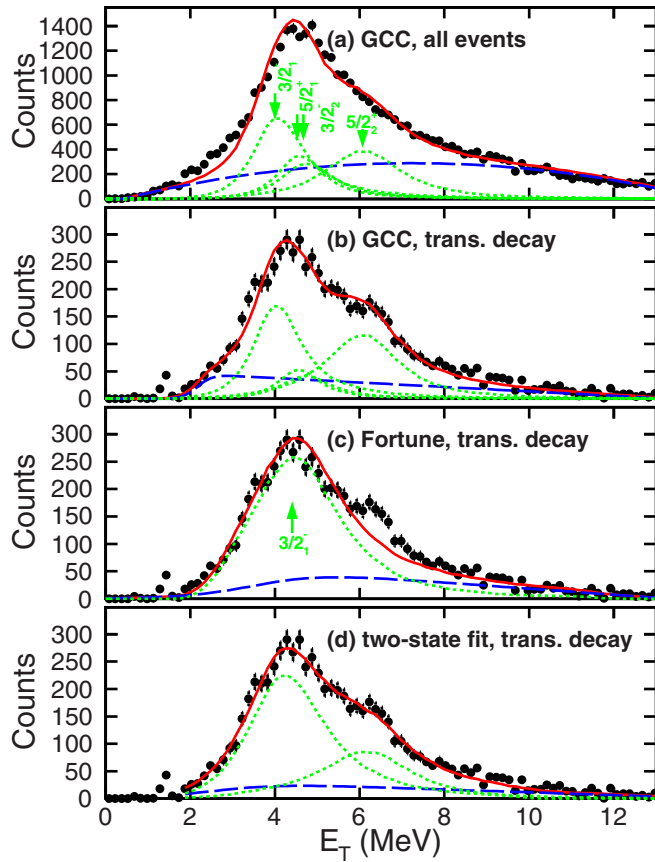
FIG. 1. Fits to the experimental $^{11}O \rightarrow 2p + {}^9C$ decay-energy spectra obtained with the invariant-mass method with (a) all experimental events and (b)–(d) for the events where the core is emitted transversely from the moving parent fragment. The solid red curves show fits to these spectra with contributions from the states shown as the dotted green curves and a background component given by the dashed blue curves. The fit in panels (a), (b) includes the contributions from the $3/2_1^-$, $3/2_2^-$, $5/2_1^+$, and $5/2_2^+$ states predicted in the GCC. In panel (c), the fit includes only the ground-state peak as predicted by Fortune [3]. The fit in panel (d) is a two-peak fit using R-matrix lineshapes for diproton emission, with both widths and centroids varied. The data and fits in panel (a) are the same as presented in Ref. [1] where it was incorrectly stated in the figure caption that a transverse gate was applied.

and width of each of the states were obtained from the GCC calculation.

These peaks can be moved collectively along the energy axis by adjusting the depth of the $p - {}^9C$ potential in the GCC model. The spectrum in Fig. 1(a) is the best fit obtained by varying this depth and allowing the relative intensities of the four levels to vary. The effect of the detector resolution and the E_T-dependent efficiency has been included in this fit by using Monte Carlo simulations of the reaction [1]. A smooth background was assumed in this fit, which is parametrized as a inverse Fermi function multiplied by a linear function. The parameters of this background function were also varied in the fit.

The invariant-mass resolution in p and $2p$ decay in experiments with HiRA has been shown to be largely determined by the effects associated with energy loss of the decay fragments in the target material [9,10]. Specifically, the cores (^9C in this case) are slowed down more than the protons, thus changing their relative velocities and the invariant mass. While an average correction is made by assuming that the decay occurred at half the target depth, the contributions from different decay depths dominate the invariant-mass resolution. In Refs. [9,10] it was shown that the invariant-mass resolution can be improved by restricting events to those where the core is emitted close to 90 degrees, i.e., transversely, in the reference frame of the decaying parent. Such gates were applied in the analysis of the ^{12}O invariant mass in Ref. [2]. It is thus desirable to now include such gates for the analysis of ^{11}O.

Figure 1(b) shows the transverse-gated spectrum for ^{11}O where $|\cos\theta_c| < 0.2$ and θ_c is the emission angle in the parent's reference frame and $\theta_c = 0$ corresponds to the beam axis. This spectrum shows more structure than the ungated spectrum in Fig. 1(a) with the emergence of a small bump, or shoulder, on the high-energy side of the peak at $E_T \approx 6.4$ MeV. This bump occurs close to the predicted location of the second $5/2^+$ state in the GCC fit. The solid red curve in Fig. 1(b) is fit with the same ingredients as the original fit, except the experimental resolution and efficiency in the Monte Carlo simulations are modified to include the transverse gate. The relative contribution from each of the four peaks is quite similar to our fit of the ungated spectrum in Fig. 1(a). However, we note that the $3/2_2^-$ and $5/2_1^+$ states are nearly degenerate in both fits, so a three-peak fit would give a similar level of reproduction.

To further highlight that the observed peak is a multiplet, we have taken the lineshape predicted by Fortune for the ground state (solid curve in Fig. 1 of Ref. [3]), incorporated the experimental resolution and the E_T-dependent detection efficiency, and fit the experimental data with the same background parametrization. The result is shown in Fig. 1(c), where most of the experimental spectrum can be reproduced except for the region of the bump. A second state, at least, must be present in order to fit the full spectrum.

Figure 1(d) shows a two-peak fit using lineshapes taken from R-matrix theory [11] for diproton emission with the $p - p$ relative energy fixed to zero for simplicity. The centroid and widths of the ground and excited states from the poles of their S matrix are $E_T = 4.25(6)$ MeV, $\Gamma = 2.31(14)$ MeV and $E_T = 6.40(7)$ MeV, $\Gamma = 2.5(4)$ MeV, respectively. At this ground-state energy, the GCC prediction for the ground-state width is $\Gamma = 1.29$ MeV but could be envisaged to increase to ≈ 1.9 MeV if the ground-state configuration is pure $(s_{1/2})^2$ [1]. The latter width approaches the fitted value of 2.31(14) MeV in our two-peak fit, but the preferred interpretation in the GCC requires the presence of at least one other state. This fitted ground-state width is consistent with the value of 2.46 MeV predicted by Fortune for simultaneous $2p$ decay alone.

If the "bump" in the E_T spectrum is associated with the $5/2_2^+$ state, as suggested by the GCC model, then Fortune's arguments that only the ground state should be excited in a $2n$-knockout reaction are incorrect. Possibly Fortune's structure
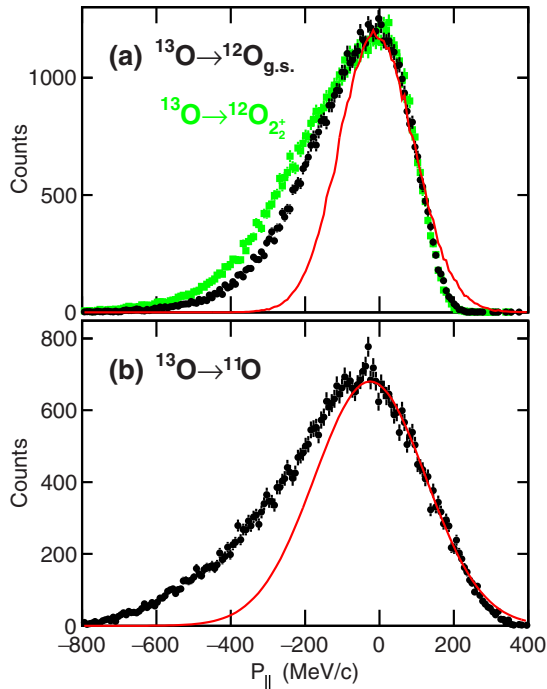
FIG. 2. Experimental longitudinal-momentum distributions of reconstructed residuals following (a) $1n$ and (b) $2n$ knockout from the ^{13}O projectile. In panel (a), results are presented gated on the two indicated states in ^{12}O, while in panel (b), the data are for all $2p + {}^9$C events in the invariant-mass peak. The longitudinal momentum is determine in the frame of the projectile at its velocity in the center of the target. The curve in panel (a) is a prediction with the eikonal model (with same ingredients as in Ref. [12]) normalized to the experimental peak height and the experimental resolution included via Monte Carlo simulations. It roughly reproduces the experimental data at the higher momenta. The curve in panel (b) is a Gaussian fit to the high-momentum data above the maximum to highlight the asymmetry of the experimental data.

model is too simplistic, or the reaction mechanism is more complex than assumed. At the bombarding energies of this work, theoretical treatments of single-nucleon knockout often invoke the sudden approximation with an eikonal treatment [13]. The predicted longitudinal-momentum $P_{\parallel}$ distributions of the projectile residuals are symmetric in shape and the width is characterized by the angular momentum of the removed nucleon. In Fig. 2(a) the extracted distribution for the ground and 2_2^+ states ^{12}O are shown for the one-neutron-knockout reaction, where the momentum is determined from the center of mass of the $2p + {}^{10}$C decay products. These two distributions are very similar to each other but are far from symmetric in shape with a significant tailing to smaller momenta. This is highlighted by the symmetric curve in Fig. 2(a), which is a calculation using the eikonal model and where the experimental resolution is folded in. This curve reproduces the high-momentum region rather well, except for the very highest momentum where the model is expected to fail because it does not conserve momentum [14]. Based on the observations in Ref. [14], the distribution may be expected to have a narrow peak-like structure at the maximum possible

momentum of $P_{\parallel} = 154$ MeV/c (4427 MeV in the laboratory frame) in Fig. 2(a). However, due to the large momentum resolution of 100 MeV/c (FWHM) in this measurement, any such structure would be washed out. Low-momentum tails have been observed in a number a knockout reactions [14–18], but the magnitude of the tail in this instance is more significant than most cases, but not unprecedented [16].

The equivalent distribution for two-neutron knockout associated with our observed ^{11}O peak is shown in Fig. 2(b). Here, to highlight the asymmetry we have just fit a Gaussian curve to the high-momentum region. The $2n$-knockout distribution is wider than the $1n$ distributions in Fig. 2(a), which would be expected if the total angular momentum of the two knocked out neutrons is nonzero [19], but it also has a significant low-momentum tail. This asymmetry has been ascribed to the dynamics of the removed nucleon inside the potential of the residual nucleus [14,20] or caused by dissipative knockout reactions. The latter can involve excitation of either the target nucleus or the core or both. A reduction in the residual momentum of 100 MeV/c corresponds to a dissipation of ≈ 30 MeV into excitation energy. While such large dissipations maybe dominating the tail regions, it is not clear whether smaller dissipations also contribute to the high-momentum region of the distribution. We note that the "bump" in the ^{11}O invariant-mass distribution does not disappear when gated on $P_{\parallel}$ values above the peak in the momentum spectrum. Whether dissipative knockout reactions are responsible for the production of the $5/2_2^+$, and possibly the other low-lying excited states, is not clear. Further understanding of these reactions is needed.

Finally, we note that the efficiency-corrected yield in the ^{11}O invariant-mass peak is of similar magnitude as those determined for the observed $1n$-knockout states in Ref. [2]. In fact, this yield is 34% larger than the $1n$-knockout yield to ^{12}O$_{g.s.}$. In addition, the second observed 2^+ state in ^{12}O has a yield of about twice the observed yield of the ^{11}O peak. Given that the cross section for knockout of a deeply bound neutron is expected to be small [12], the $2n$ yield is expected to be significantly smaller. If the observed peak has contributions from four states of similar magnitude as suggested in the GCC interpretation, the ^{11}O ground-state yield is closer to this expectation, but still the relative yield is significant.

In conclusion we have shown that invariant-mass spectrum of $2p + {}^9$C events produced in the $2n$ knockout from an ^{13}O beam cannot be understood as the production and decay of a single ^{11}O state as suggested by Fortune [3]. A high-energy shoulder or bump can be resolved in this spectrum when a selection of events associated with transversely emitted cores is applied. The location of this bump is consistent with contribution of the $5/2_2^+$ state predicted in Gamow coupled-channels calculations. However, the data are not able to differentiate between the ground-state location and width predicted in the Gamow coupled-channels model and the simultaneous $2p$-decay calculations of Fortune.

[1] T. B. Webb, S. M. Wang, K. W. Brown, R. J. Charity, J. M. Elson, J. Barney, G. Cerizza, Z. Chajecki, J. Estee, D. E. M. Hoff *et al.*, First Observation of Unbound ^{11}O, the Mirror of the Halo Nucleus ^{11}Li, Phys. Rev. Lett. **122**, 122501 (2019).

[2] T. B. Webb, R. J. Charity, J. M. Elson, D. E. M. Hoff, C. D. Pruitt, L. G. Sobotka, K. W. Brown, J. Barney, G. Cerizza, J. Estee *et al.*, Particle decays of levels in ^{11,12}N and ^{12}O investigated with the invariant-mass method, Phys. Rev. C **100**, 024306 (2019).

[3] H. T. Fortune, Energy and width of ^{11}O(g.s.), Phys. Rev. C **99**, 051302(R) (2019).

[4] H. T. Fortune, Population of ^{11}O* in two-neutron removal from ^{13}O, Phys. Rev. C **100**, 024332 (2019).

[5] S. M. Wang, W. Nazarewicz, R. J. Charity, and L. G. Sobotka, Structure and decay of the extremely proton-rich nuclei ^{11,12}O, Phys. Rev. C **99**, 054302 (2019).

[6] H. T. Fortune, 2p decays of ^{11}O, Phys. Rev. C **96**, 014317 (2017).

[7] S. M. Wang and W. Nazarewicz (unpublished).

[8] M. S. Wallace, M. A. Famiano, M.-J. van Goethem, A. M. Rogers, W. G. Lynch, J. Clifford, F. Delaunay, J. Lee, S. Labostov, M. Mocko, L. Morris *et al.*, The high resolution array (HiRA) for rare isotope beam experiments, Nucl. Instrum. Methods Phys. Res., Sect. A **583**, 302 (2007).

[9] R. J. Charity, K. W. Brown, J. Elson, W. Reviol, L. G. Sobotka, W. W. Buhro, Z. Chajecki, W. G. Lynch, J. Manfredi, R. Shane *et al.*, Invariant-mass spectroscopy of ^{18}Ne, ^{16}O, and ^{10}C excited states formed in neutron-transfer reactions, Phys. Rev. C **99**, 044304 (2019).

[10] R. J. Charity, K. W. Brown, J. Okołowicz, M. Płoszajczak, J. M. Elson, W. Reviol, L. G. Sobotka, W. W. Buhro, Z. Chajecki, W. G. Lynch *et al.*, Invariant-mass spectroscopy of ^{14}O excited states, Phys. Rev. C **100**, 064305 (2019).

[11] A. M. Lane and R. G. Thomas, *R*-matrix theory of nuclear reactions, Rev. Mod. Phys. **30**, 257 (1958).

[12] J. A. Tostevin and A. Gade, Systematics of intermediate-energy single-nucleon removal cross sections, Phys. Rev. C **90**, 057602 (2014).

[13] P. G. Hansen and J. A. Tostevin, Direct reactions with exotic nuclei, Annu. Rev. Nucl. Part. Sci. **53**, 219 (2003).

[14] F. Flavigny, A. Obertelli, A. Bonaccorso, G. F. Grinyer, C. Louchart, L. Nalpas, and A. Signoracci, Nonsudden Limits of Heavy-Ion Induced Knockout Reactions, Phys. Rev. Lett. **108**, 252501 (2012).

[15] J. A. Tostevin, D. Bazin, B. A. Brown, T. Glasmacher, P. G. Hansen, V. Maddalena, A. Navin, and B. M. Sherrill, Single-neutron removal reactions from ^{15}C and ^{11}Be: Deviations from the eikonal approximation, Phys. Rev. C **66**, 024607 (2002).

[16] A. Gade, D. Bazin, C. A. Bertulani, B. A. Brown, C. M. Campbell, J. A. Church, D. C. Dinca, J. Enders, T. Glasmacher, P. G. Hansen *et al.*, Knockout from ^{46}Ar : $\ell = 3$ neutron removal and deviations from eikonal theory, Phys. Rev. C **71**, 051301(R) (2005).

[17] G. F. Grinyer, D. Bazin, A. Gade, J. A. Tostevin, P. Adrich, M. D. Bowen, B. A. Brown, C. M. Campbell, J. M. Cook, T. Glasmacher *et al.*, Knockout Reactions from p-Shell Nuclei: Tests of *Ab Initio* Structure Models, Phys. Rev. Lett. **106**, 162502 (2011).

[18] R. Shane, R. J. Charity, L. G. Sobotka, D. Bazin, B. A. Brown, A. Gade, G. F. Grinyer, S. McDaniel, A. Ratkiewicz, D. Weisshaar, A. Bonaccorso, and J. A. Tostevin, Proton and neutron knockout from ^{36}Ca, Phys. Rev. C **85**, 064612 (2012).

[19] E. C. Simpson, J. A. Tostevin, D. Bazin, and A. Gade, Longitudinal momentum distributions of the reaction residues following fast two-nucleon knockout reactions, Phys. Rev. C **79**, 064621 (2009).

[20] K. Ogata, K. Yoshida, and K. Minomo, Asymmetry of the parallel momentum distribution of (p, pn) reaction residues, Phys. Rev. C **92**, 034616 (2015).